Advances in Geo-Energy Research

Vol. 13, No. 1, p. 69-80, 2024

Original article

Numerical simulation of ultrasonic wave propagation characteristics in water-based drilling fluid

Jifang Wan[1], Yanqi Zhao[2], Yuanhua Zhou[2]*, Jingcui Li[1], Shengwei Dong[3], Peng Sun[4]

[1] China Energy Digital Technology Group Co., Ltd., Beijing 100044, P. R. China
[2] School of Mechanical Engineering, Yangtze University, Jingzhou 434023, P. R. China
[3] CNPC Engineering Technology R&D Company Limited, Beijing 102200, P. R. China
[4] Sinopec Research Institute of Petroleum Engineering Co., Ltd., Beijing 102206, P. R. China

Keywords:
Ultrasonic
drilling fluid
solid phase particle
propagation characteristics
numerical simulation

Cited as:
Wan, J., Zhao, Y., Zhou, Y., Li, J., Dong, S., Sun, P. Numerical simulation of ultrasonic wave propagation characteristics in water-based drilling fluid. Advances in Geo-Energy Research, 2024, 13(1): 69-80.
https://doi.org/10.46690/ager.2024.07.08

Abstract:
Ultrasonic wave propagates with strong penetration, high stability, and has non-contact nature, therefore it is widely used in the petroleum industry. As an application example, an ultrasonic flowmeter can accurately measure the annular flow rate of water-based drilling fluid. According to the outlet flow rate, it can be noticed if there is an abnormal situation in the well to avoid accidents such as well kick and blowout. However, due to the attenuation of ultrasonic wave in the drilling fluid, the relevant research results are not reliable. Herein, based on the theory of acoustics, the influences of water-based drilling fluid density, solid particle size and solid particle number on the ultrasonic attenuation characteristics under different frequencies are studied by numerical simulation. First, the propagation characteristics of ultrasonic wave in water-based drilling fluid are systematically analyzed, then the accuracy of the above results is verified by laboratory tests. The results show that the ultrasonic attenuation rate is positively correlated with the solid particle size, solid particle number and ultrasonic frequency in water-based drilling fluid, while it is negatively correlated with the density of water-based drilling fluid. Furthermore, it is established that the ultrasonic energy decreases with increasing propagation distance. The results of this study can provide a theoretical basis and practical guidance for using an ultrasonic flowmeter to accurately measure the annulus return flow rate of drilling fluid and develop an intelligent drilling system, so as to improve the efficiency of field operation and drilling success rate.

1. Introduction

The outlet flow rate of the drilling fluid is a crucial parameter in field drilling operations (Wang and Zheng, 2021). Based on the change characteristics of outlet flow, some abnormal situations that may occur underground can be detected, such as blowout and well kick (Korlapati et al., 2022). The accuracy and timeliness of flow monitoring methods used in field drilling have an important influence on the judgment of underground accidents (Li et al., 2022a). If the export flow cannot be monitored quickly and accurately, this will lead to the misjudgment of underground accidents. However, such accidents can be effectively avoided or alleviated by the accurate monitoring of drilling fluid flow, an essential task during drilling operations (Ma et al., 2022; Indimath et al., 2024). Ultrasonic waves not only share the general characteristics of refraction and reflection of acoustic waves but also inherently have good directivity, high power, strong penetration, non-contact measurement ability, and wide frequency range, therefore are widely utilized in the flow detection of solid, liquid and gas media (Poelma, 2020).

Scholars around the world have extensively studied the propagation characteristics of ultrasonic waves in various media. As for numerical analysis, based on the Epstein-Carhar model, Allegra and Hawley (1972) proposed the European Chemicals Agency model, which is considered the

*Corresponding author.
E-mail address: wanjifang@126.com (J. Wan); zyq20000701@126.com (Y. Zhao); zhouyuanhua@yangtzeu.edu.cn (Y. Zhou); jcli3563@ceec.net.cn (J. Li); steved66@126.com (S. Dong); sunpeng.sripe@sinopec.com (P. Sun).
Yandy Scientific Press
2207-9963
Received May 24, 2024; revised June 17, 2024; accepted July 12, 2024; available online July 18, 2024.

main calculation model for the propagation and attenuation characteristics of ultrasonic wave in gas-dust flow. Peters and Petit (2000) developed a spectral method for measuring broadband frequency velocity and attenuation by means of fast Fourier transform, achieving the effective measurement of the absolute value of phase velocity as well as the attenuation coefficient of ultrasonic waves in a suspension consisting of solid-phase particles. Liu et al. (2012) studied the attenuation characteristics of ultrasonic wave in water-based drilling fluid by Urick's model and discussed the influence of propagation distance, ultrasonic frequency, liquid density, and other factors on ultrasonic attenuation. Xia et al. (2013) investigated the propagation and attenuation characteristics of ultrasonic waves in static gas containing spherical particles and proposed a corresponding theoretical model. Jia et al. (2020) employed COMSOL Multiphysics software to analyze the influence of typical factors on the accuracy of ultrasonic flow measurement and evaluated the propagation characteristics of ultrasonic wave in fluid. In terms of experimental analysis, Moradi and Abedini (2012) and Setia et al. (2015) studied the propagation law of ultrasonic wave in rock materials. Sojahrood et al. (2017) developed a nonlinear model to numerically simulate the attenuation of ultrasound and the speed of sound in a bubble medium. They concluded that changes in the attenuation and sound speed are nonlinear and depend on the frequency and pressure of the ultrasonic pulse, nonlinear oscillations of the MBs, and the interaction between the MBs. By considering the bubble-bubble interactions, the numerical results can predict the quantitative and qualitative changes in the attenuation and frequency as well as the generation of the secondary peaks. Mozie (2017) experimentally determined the amplitude attenuation coefficients of different fluid samples and compared them with the acoustic properties at different frequencies. Fan and Wang (2021) presented the principles, characteristics, application areas and research examples of different ultrasonic methods used for two-phase flow measurements, compared their advantages and disadvantages, and predicted future trends. Holt et al. (2020) investigated the phenomenon of borehole collapse during drilling in shale formations and experimentally verified that ultrasonic velocity, especially attenuation measurements, are sensitive to the initiation process of damage. They also provided values of isotropic velocity and longitudinal wave impedance, which allows for the monitoring of rock state.

In summary, many scholars have adopted the Urick model, Epstein-Carhar model, European Chemicals Agency model, and used COMSOL Multiphysics software, both in terms of numerical simulation and experiment (Özkök, 2017; Ge et al., 2022; Leśniak et al., 2022). Several studies have also focused on the propagation characteristics of ultrasonic wave in drilling fluid, while the factors considered were relatively simple or the study was relatively broad, which cannot accurately reflect the influence of different factors on the propagation of ultrasonic wave in drilling fluid (Chen et al., 2019; Li et al., 2022b). In this paper, water-based drilling fluid is taken as the propagation medium, and a combination of theoretical analysis, numerical simulation and laboratory test is applied. The effects of water-based drilling fluid density, solid particle size, and solid particle number on ultrasonic attenuation at different frequencies are studied, and the propagation characteristics of ultrasonic are summarized. The findings of this paper can provide a useful theoretical framework for using an ultrasonic flowmeter to accurately measure the circumferential return flow of water-based drilling fluid, with the aim to avoid the occurrence of blowout, well kick, and other accidents, and reduce the likelihood of complex downhole accidents. Moreover, this work lays the theoretical basis and provides practical guidance for the development of intelligent drilling systems, helping to improve the efficiency of field operation and drilling success rate.

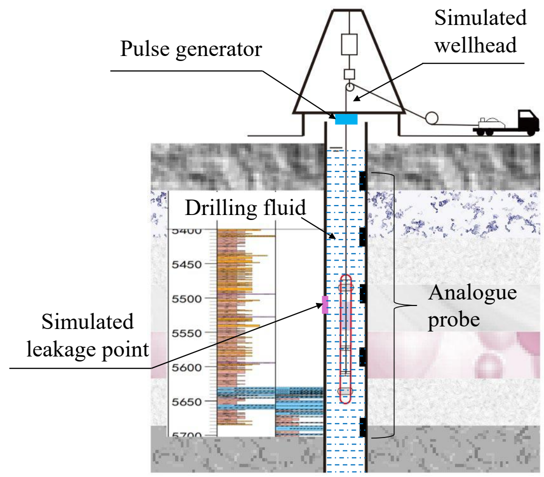

Fig. 1. Schematic diagram of ultrasonic testing.

2. Analysis of propagation theory

2.1 Propagation equation

During ultrasonic wave transmission in water-based drilling fluid, due to the fluid having a certain viscosity, ultrasonic energy is attenuated. Therefore, when studying the transmission law of an ultrasonic signal in water-based drilling fluid, it is necessary to understand the propagation process and attenuation law of ultrasonic waves in such fluid. Three main types of ultrasonic attenuation have been described, such as diffusion attenuation, scattering attenuation and viscosity attenuation (Peruga, 2021). The field principle of ultrasonic testing drilling fluid in oil and gas wells is shown in Fig. 1.

In the process of ultrasonic wave propagation in water-based drilling fluid, the wave amplitude changes with the number of solid particles, the particle size of solid particles, and the density of the drilling fluid (Zhu et al., 2023). According to the theory of acoustics (Morse and Ingard, 1986), when the ultrasonic wave propagates in a medium to a distance of x, the change in its sound intensity can be expressed by the following formula:

$$I_L = I_0 e^{-\alpha x} \tag{1}$$

where I_L represents the sound intensity of ultrasonic waves during propagation in the medium, W/m^2; I_0 represents the initial sound intensity, W/m^2; α represents the attenuation coefficient of ultrasonic wave in the medium, dimensionless;

x is the propagation distance, m.

From Eq. (1), it can be deduced that when the ultrasonic wave propagates in the medium, the change in ultrasonic wave energy is closely related to the attenuation coefficient α.

2.1.1 Diffusion attenuation

Diffusion attenuation refers to the phenomenon that in the process of ultrasonic propagation, the sound speed of non-plane waves increases continuously with increasing propagation distance, which is accompanied with the sound pressure on unit area gradually decreasing (Peruga, 2021). The occurrence of diffusion attenuation phenomenon is only related to the propagation distance of ultrasonic wave and has nothing to do with other parameters. The diffusion attenuation coefficient is a fixed value; therefore, the influence of diffusion attenuation on ultrasonic wave propagation is not considered in this paper.

2.1.2 Scattering attenuation

When propagating in a liquid medium, the ultrasonic wave will be interfered by solid particles in the water-based drilling fluid, resulting in scattering attenuation. This phenomenon causes part of the ultrasonic wave to be deflected into the surrounding environment, resulting in its decreased acoustic intensity (Peruga, 2021). The degree of scattering attenuation is not only related to the number and particle size of solid particles in the water-based drilling fluid but also closely linked to the characteristics of water-based drilling fluid itself. To facilitate theoretical research, it is necessary to assume that the solid phase particle of the water-based drilling fluid is a rigid spherical object (Kuang et al., 2023). Assuming that the radius of such particle is r, in this state, the scattering attenuation coefficient will be:

$$\alpha_s = \frac{2}{9} N m^4 \pi r^6 \tag{2}$$

where α_s represents the scattering attenuation coefficient, dimensionless; N represents the number of solid particles per unit volume, dimensionless; m represents the wave number of ultrasonic wave, dimensionless; r represents the radius of the solid-phase particles, m.

2.1.3 Viscosity attenuation

Viscosity attenuation is mainly due to the friction force arising from the difference in the velocities of adjacent particles in a liquid medium. In addition, in the water-based drilling fluid, there is a heat conduction phenomenon, that is, heat transfer between particles. Due to the different densities of water-based drilling fluid, the heat generated during the stress process will also be different, resulting in attenuation. Several authors have highlighted that the relationship between the density and viscosity coefficient of water-based drilling fluid can be obtained by the Urick-Lamb formula (Seldis and Pecorari, 2000; Matsushima et al., 2011; Larrarte and François, 2012). The calculation formula of the viscosity coefficient (α_v) is:

$$\alpha_v = \frac{3}{8} \pi m r \frac{q(h-1)^2}{q^2 + (h+j)^2} \tag{3}$$

$$q = \frac{4}{9re}\left(1 + \frac{1}{re}\right) \tag{4}$$

$$j = \frac{1}{2} + \frac{9}{4re} \tag{5}$$

$$e = \sqrt{\frac{b}{2g}} \tag{6}$$

where b represents the angular frequency, rad/s; g represents the viscosity of water; h represents the ratio of particle density to liquid density of water-based drilling fluid, dimensionless (Peruga, 2021); q is related to the parameter e and r, dimensionless; j is dimensionless constant derived from e and r and including a numerical factor, dimensionless; e is a factor involving the square root of the ratio of angular frequency b to twice the viscosity of water g, dimensionless.

2.2 Calculation results and analysis

Water-based drilling fluids can be characterized by rheological properties, temperature stability, and leaching properties, and are commonly used for sampling. For the purpose of this study, the solid particle size is taken as 100-270 mesh (about 50-175 μm) (Li et al., 2019), the solid particle density is 2.4-3.0 g/cm^3, and the density of water-based drilling fluid is 1.02-1.34 g/cm^3 (Ismail, 2014; Broni-Bediako and Amorin, 2019).

2.2.1 Numerical simulation of scattering attenuation

According to the formula of scattering attenuation coefficient, the main factors affecting the attenuation coefficient are ultrasonic frequency, solid particle size and solid particle number.

In this simulation, the particle size of water-based drilling fluid is set to change from 5×10^{-6} to 5×10^{-5} m (Li et al., 2019). Six ultrasonic wave frequencies are set, namely, 0.1, 0.2, 0.3, 0.4, 0.5 and 0.6 MHz (Liu et al., 2012). The number of solid particles is 10^{14} (Ismail, 2014; Broni-Bediako and Amorin, 2019). Numerical simulation is carried out by Matlab software to study the scattering attenuation coefficient of ultrasonic wave in water-based drilling fluid. Fig. 2 shows the relationship between the solid particle size and the scattering attenuation coefficient in the water-based drilling fluid under different ultrasonic frequencies.

As shown in Fig. 2, under a constant frequency of the ultrasonic wave, its scattering attenuation coefficient increases gradually with the increase in the solid particle size in the water-based drilling fluid, and it is proportional to the cubic of the solid particle size of the water-based drilling fluid (Ma et al., 2019). However, when the solid particle size of the water-based drilling fluid is less than 2×10^{-5}, the scattering attenuation can be essentially ignored. At the same time, it can be found that when the size of solid particles is constant, the scattering attenuation coefficient increases with the rising ultrasonic frequency.

When the ultrasonic frequency changes, the size of solid particles in the water-based drilling fluid is kept at 3×10^{-5} m, and the number of solid particles changes from 10^{12} to 10^{17}. The relationship curve between the number of solid-phase particles in the water-based drilling fluid and the scattering

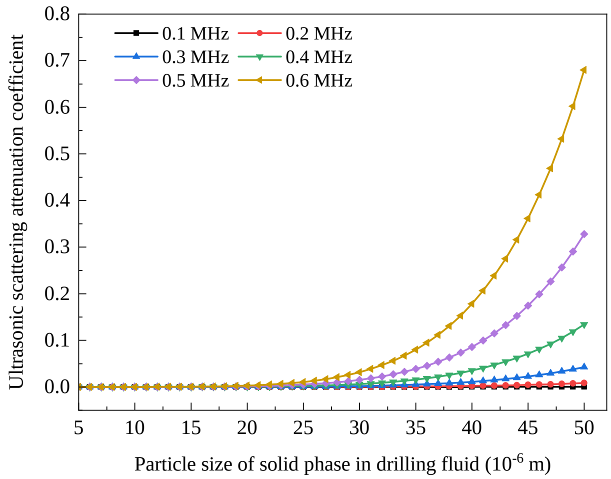

Fig. 2. Relationship between the solid particle size and the scattering attenuation coefficient.

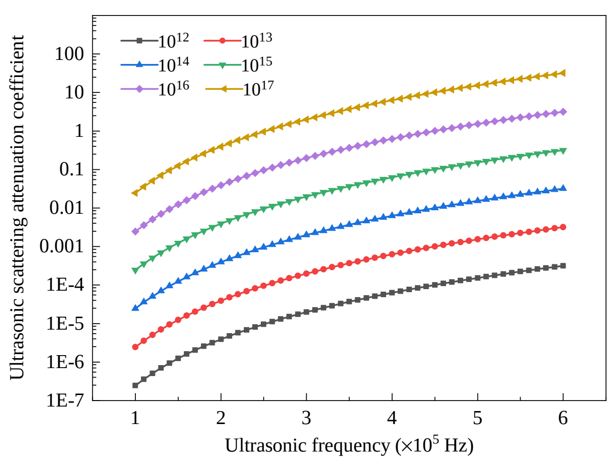

Fig. 3. Relationship between the ultrasonic frequency and the scattering attenuation coefficient.

attenuation coefficient is basically the same as that in Fig. 2, which will not be repeated here, and the relationship curve between the ultrasonic frequency and the scattering attenuation coefficient is shown in Fig. 3.

From the relationship between the number of solid-phase particles and the scattering attenuation factor, under a constant ultrasonic frequency, the attenuation coefficient of ultrasonic wave increases with the number of solid particles in the drilling fluid. However, when the number of solid particles is less than 10^{15}, the scattering attenuation can be ignored. On the other hand, when the number of solid particles is greater than 10^{15}, the number of solid particles has a great influence on the scattering attenuation coefficient of ultrasonic wave. Furthermore, when taking a fixed number of solid particles, as the acoustic frequency increases, the corresponding ultrasonic attenuation coefficient also increases gradually.

The curves for the number of particles of different solid phases are illustrated in Fig. 3. It can be seen that under a constant ultrasonic frequency, the ultrasonic attenuation coefficient increases with the increasing number of solid particles. Additionally, when the number of solid particles in the water-based drilling fluid increases by one order of magnitude, the corresponding ultrasonic scattering attenuation coefficient also increases by one order of magnitude.

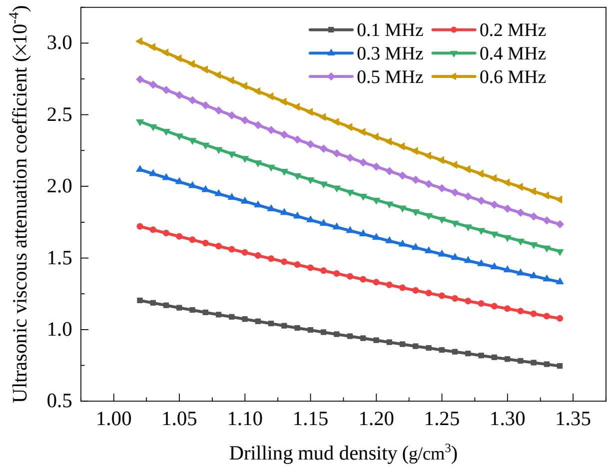

Fig. 4. Relationship between the density and viscosity attenuation coefficient of the water-based drilling fluid.

2.2.2 Numerical simulation of viscous attenuation

According to the formula of viscosity attenuation coefficient, the main factors affecting the viscosity attenuation coefficient are ultrasonic frequency, the density of water-based drilling fluid, and the particle size of the solid phase.

In this part, the relationship between the density of water-based drilling fluid and the viscosity attenuation coefficient is studied first. The ultrasonic frequency is set at 0.1, 0.2, 0.3, 0.4, 0.5 and 0.6 MHz. The water-based drilling fluid has a density of 1.02-1.34 g/cm^3, the particle size of the solid phase is 3×10^{-5} m, the density of water is 1 g/cm^3, and the viscosity of water is 1.006×10^{-6} m^2/s. To analyze the viscosity attenuation coefficient of ultrasonic wave in the water-based drilling fluid, numerical simulation is carried out by Matlab software. The relationship between the density and viscosity attenuation coefficient of the water-based drilling fluid under different ultrasonic frequencies is shown in Fig. 4.

As can be seen from Fig. 4, when the solid particle size of water-based drilling fluid is constant, the viscosity attenuation coefficient of ultrasonic wave is inversely proportional to the density of water-based drilling fluid, that is, with the increasing density of water-based drilling fluid, the viscosity attenuation coefficient of ultrasonic wave decreases. This is because with a higher density of water-based drilling fluid, the stiffness of the whole drilling fluid system also increases. As a result, the energy exchange and transmission of ultrasonic waves in rigid media becomes easier, thus its viscosity attenuation coefficient gradually dwindles. This also explains why the propagation effect of ultrasonic wave in solid matter is better than that liquid and air and its transmission distance is farther (Sheen et al., 1988). However, when the density of water-based drilling fluid is constant, the viscosity coefficient of ultrasonic wave

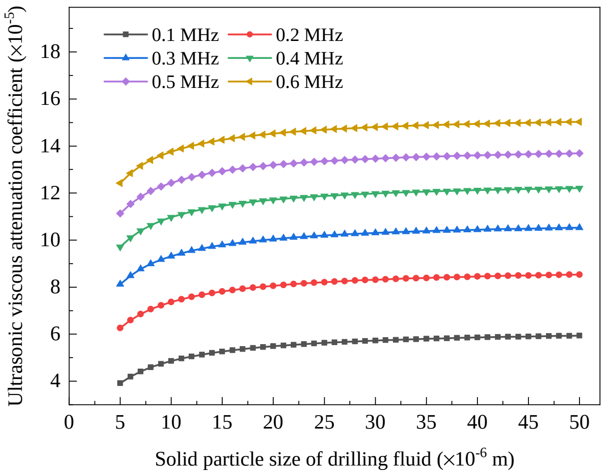

Fig. 5. Relationship between the solid particle size and the viscous attenuation coefficient.

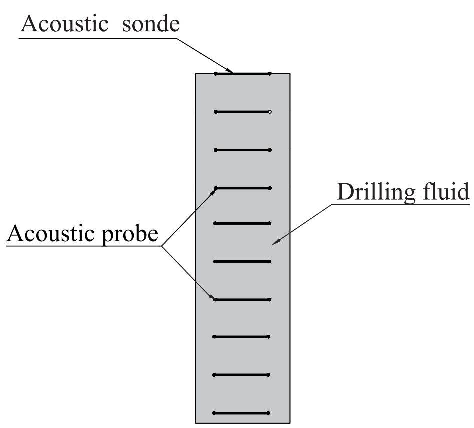

Fig. 6. Fluid domain model of the drilling fluid.

increases gradually with rising ultrasonic frequency.

Under different ultrasonic frequencies, the density of water-based drilling fluid is 1.2 g/cm^3, and the particle size of solid particles in water-based drilling fluid is from 5×10^{-6} to 5×10^{-5} m. The relationship between the size of solid particles in water-based drilling fluid and the corresponding scattering attenuation coefficients are shown in Fig. 5.

As presented in Fig. 5, under a constant density of water-based drilling fluid, the ultrasonic viscosity attenuation coefficient increases gradually with the increase in solid particle size. When the solid particle size is less than 1.5×10^{-5} m, the ultrasonic viscosity attenuation coefficient increases obviously with the increase in water-based drilling fluid particle size. However, when the solid particle size of the water-based drilling fluid is greater than 1.5×10^{-5} m, the growth trend of ultrasonic viscosity attenuation coefficient decreases obviously with the increase in water-based drilling fluid particle size. When the solid particle size of water-based drilling fluid is constant, the ultrasonic viscosity attenuation coefficient enlarges with rising ultrasonic frequency. In general, however, the viscous attenuation coefficient of ultrasonic wave is very small, even negligible.

3. Numerical simulation

The essence of studying the propagation characteristics of ultrasonic wave in water-based drilling fluid is to establish the propagation model of ultrasonic wave in a borehole. Numerical simulation mainly considers the influence of the density of water-based drilling fluid and analyzes the variation characteristics of sound pressure and the frequency of ultrasonic wave on the sound pressure during propagation. As for the propagation of ultrasonic waves, the main modeling methods are Angular Spectrum Method (ASM), Rayleigh Integration Method (RIM), Multivariate Gaussian Method (MGM), Finite Element Method (FEM), and Spatial Impulse Response Method (SIRM).

The FEM is a numerical calculation method commonly used in various engineering fields, which is also suitable for sound field research (Shahzamanian et al., 2021). Citarella et al. (2007) combined the finite element method and the boundary element method to solve the acoustic problems in structural vibration. Yasui et al. (2007) utilized the finite element method to study the relationship between the acoustic wave attenuation factor and the reactor amplitude in a sonochemical reactor. Zhang et al. (2020) employed the finite element method to simulate the surface wave in a cylinder for the first time, and the simulation results were verified by the dynamic photoelastic method. The finite element method can also be used to simulate the propagation of acoustic waves in inhomogeneous media. Therefore, to improve the accuracy of ultrasonic propagation simulation in water-based drilling fluid, this paper uses the finite element method for simulation.

3.1 Modeling

COMSOL Multiphysics software is used to simulate and analyze the propagation characteristics of ultrasonic waves in water-based drilling fluid. Considering the computing demand and the calculation time requirement, this paper takes a two-dimensional model to simulate the ultrasonic wave. The propagation characteristics of ultrasonic wave in drilling fluid are subsequently studied, where the ultrasonic wave is excited by piezoelectric force, so the numerical simulation considers each of the piezoelectric, electrostatic and circuit multi-physical fields in solid mechanics. The diameter of the drill pipe, drilling hole and upper acoustic probe is 4 inches, 8.5 inches and 30 mm, respectively, the ultrasonic frequency is set to 0.3 MHz, the acoustic probe is set at every 40 mm in the vertical direction, and the size of the fluid field of the water-based drilling fluid is 57.15 mm × 380 mm, as shown in Fig. 6.

The ultrasonic transducer is a cylindrical longitudinal wave probe with a diameter of 30 mm. The excitation signal is 0.3 MHz, and the excitation waveform signal function is expressed as:

$$an_1(t) = 1 \times 10^{-6} gp_1(t) \sin(2\pi f_0 t) \tag{7}$$

$$gp_1(t) = Ae^{\frac{-(t-t_0)^2}{2\sigma^2}} \tag{8}$$

where $an_1(t)$ represents the function of amplitude with time; t represents the independent variable time, s; $gp_1(t)$ represents

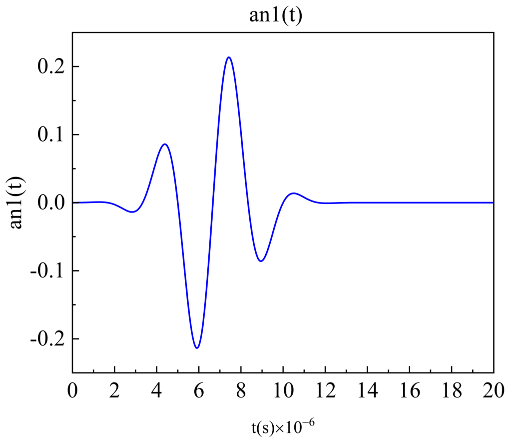

Fig. 7. Excitation signal.

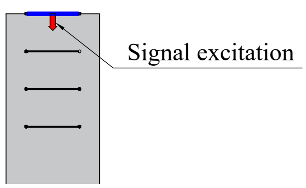

Fig. 8. Signal excitation position.

the Gaussian pulse signal, A represents the peak value of the Gaussian pulse signal, V; t_0 represents the centre time, s; σ represents the width of the marked pulse, m; f_0 is the ultrasonic frequency, MHz.

In order to simulate the ultrasonic longitudinal wave transducer and thus the signal excitation, normal velocity is added to the 30 mm line segment. The excitation signal is the Gaussian pulse shown in Fig. 7, and the signal excitation position is presented in Fig. 8.

Due to the large size of the model, to reduce the running time and improve the computational efficiency, the maximum grid of the fluid domain is set to 1/6 wavelength, and the free quadrilateral grid is taken to generate a total of 31,415 domain units and 1,340 boundary units.

In general, when solving the finite element model, to ensure the accuracy of the solution, it is necessary to set the time step of the solver. Selecting a larger step does not meet the requirements of the calculation accuracy, and the calculation effect will deviate from the actual results, while selecting a smaller step will increase the cost and reduce the efficiency of the calculation. By means of testing, the time step of this model is determined as:

$$\Delta t = \frac{T_0}{35} \tag{9}$$

where Δt represents the time step, s; T_0 represents the ultrasonic period, dimensionless.

3.2 Simulation results and analysis

The different densities of water-based drilling fluid are analyzed by COMSOL Multiphysics software, and the established fluid domain model is shown in Fig. 6. After meshing, setting the boundary conditions and loading excitation, the simulation model is solved by transient calculation. In the calculation, probes are set at different positions of the model to observe the sound pressure of ultrasonic waves at corresponding positions, so that the propagation characteristics of ultrasonic waves can be studied according to the sound pressure of ultrasonic waves detected at different positions (Chen et al., 2017). The simulated sound fields of the model at 30.76, 90.09, 145.62 and 224.95 μs are shown in Fig. 9.

3.2.1 Influence of water-based drilling fluid density

Six groups of simulation tests with different water-based drilling fluid densities are set up, including 1.08, 1.12, 1.16, 1.20, 1.24 and 1.28 g/cm^3. By setting several probes, the ultrasonic sound pressure data at different densities and positions can be detected. The ultrasonic sound pressure waveforms detected by the probes under different water-based drilling fluid densities are shown in Fig. 10.

As can be seen in Fig. 10, under the same drilling fluid density, as the distance of ultrasonic propagation increases, the sound pressure of the ultrasonic wave gradually decreases. The sound pressure of ultrasonic waves at different densities but the same positions was also studied, and the ultrasonic sound pressure data detected by probes No.1-8 at different drilling fluid densities is listed in Table 1.

The curve of the sound pressure data detected by the probe at different densities is shown in Fig. 11. As can be seen from the figure, under the same water-based drilling fluid density, when the ultrasonic frequency is constant, the sound pressure of the ultrasonic wave gradually decreases with the increase in the transmission distance, that is, the ultrasonic energy attenuates.

Given the same position, under the excitation of the same frequency ultrasonic wave, with the increase in the density of water-based drilling fluid, the ultrasonic sound pressure value at this point also increases, that is, the attenuation of ultrasonic wave decreases with the increase in the density of water-based drilling fluid, the degree of which is inversely proportional to the relationship. This once again verifies that the propagation effect of ultrasonic wave in solid matter is better than that in liquid and air, and its transmission distance is farther.

3.2.2 Effect of ultrasonic frequency

For this simulation, water-based drilling fluid with a density of 1.16 g/cm^3 is selected, and ultrasonic waves of 0.1, 0.2, 0.3, 0.4, 0.5 or 0.6 MHz are used as excitation signals. Other settings remain unchanged, and the changes in ultrasonic sound pressure at different frequencies are studied. The waveforms of ultrasonic pressure detected by the lower probe at different ultrasonic frequencies are shown in Fig. 12.

Based on the figure, the ultrasonic sound pressure data detected by probes No.1-8 at different ultrasonic frequencies are listed in Table 2.

The curve of sound pressure data detected by the probe at different ultrasonic frequencies is shown in Fig. 13.

As shown in Fig. 13, given the same propagation distance in the water-based drilling fluid, the higher the frequency of the ultrasonic wave, the greater the degree of attenuation, and the attenuation of the ultrasonic wave with 0.6 MHz is the most

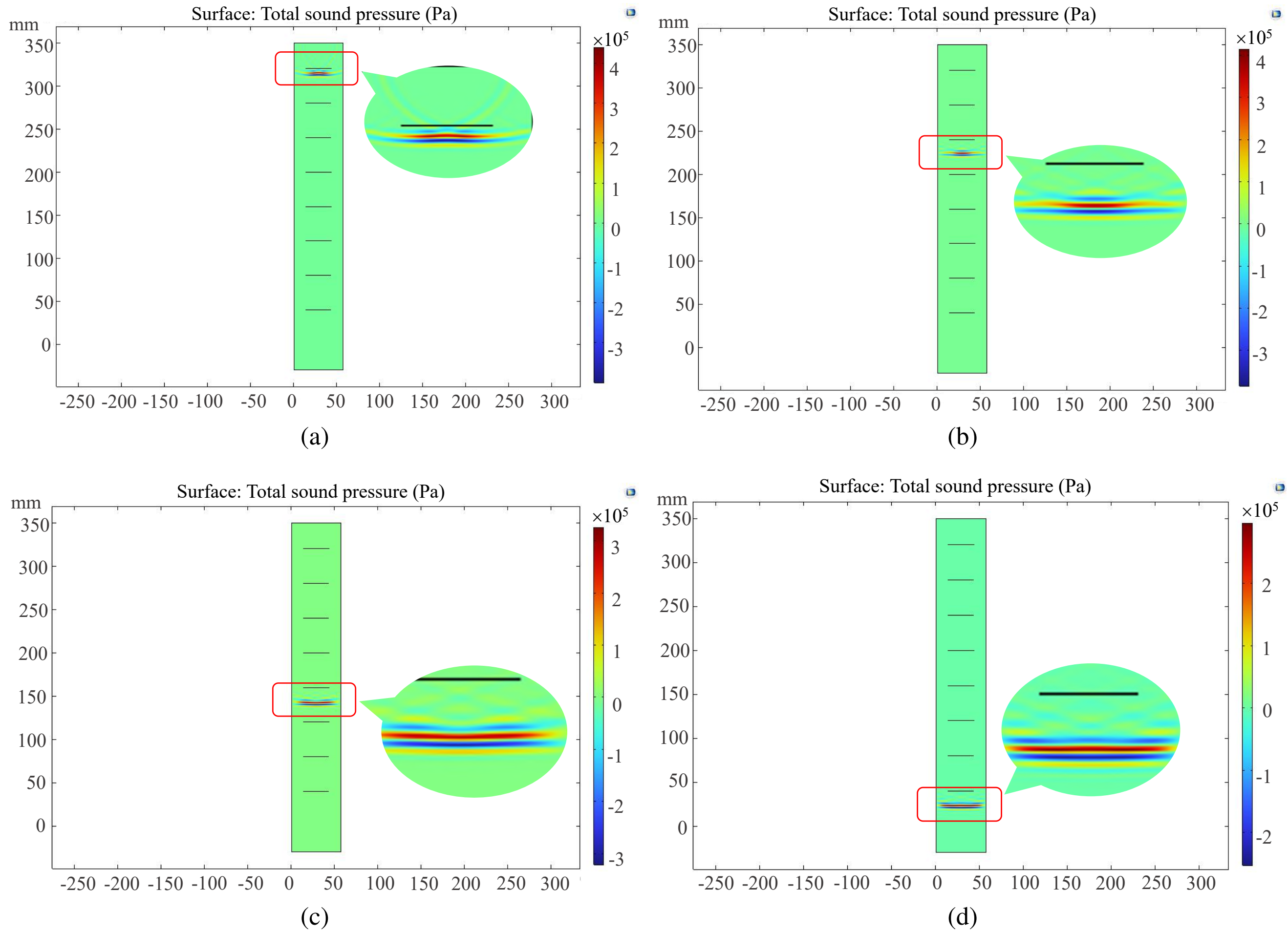

Fig. 9. Ultrasonic propagation sound field at different times. (a) 30.76µs, (b) 90.09µs, (c) 145.62µs and (d) 224.95µs.

Table 1. Ultrasonic sound pressure data detected by probes Nos.1-8 at different densities.

Density (g/cm^3)	Pressure at different propagation distance ($\times 10^5$ Pa)							
	30 (mm)	70 (mm)	110 (mm)	150 (mm)	190 (mm)	230 (mm)	270 (mm)	310 (mm)
1.08	3.19796	3.04668	2.93765	2.90457	2.86407	2.80794	2.73542	2.65688
1.12	3.31642	3.15954	3.04645	3.01216	2.97016	2.91194	2.83673	2.75228
1.16	3.48360	3.27237	3.15525	3.11974	3.07624	3.01593	2.93804	2.85368
1.20	3.55328	3.38523	3.26405	3.22733	3.18232	3.11994	3.03934	2.95209
1.24	3.67174	3.49805	3.37285	3.33487	3.28838	3.22393	3.14065	3.05049
1.28	3.79017	3.61088	3.48165	3.44246	3.39446	3.32379	3.24196	3.14890

obvious. To more intuitively describe the attenuation trend of ultrasonic waves with different frequencies in the water-based drilling fluid, the six curves from 0.1 to 0.6 MHz are respectively fitted:

$$y_1 = -0.0007703x_1 + 1.11754 \tag{10}$$

$$y_2 = -0.00128x_2 + 2.33261 \tag{11}$$

$$y_3 = -0.00185x_3 + 3.4237 \tag{12}$$

$$y_4 = -0.0025x_4 + 4.55119 \tag{13}$$

$$y_5 = -0.00441x_5 + 5.70321 \tag{14}$$

$$y_6 = -0.00614x_6 + 6.87666 \tag{15}$$

where $x_1 \sim x_6$ represents the distance of ultrasonic propa-

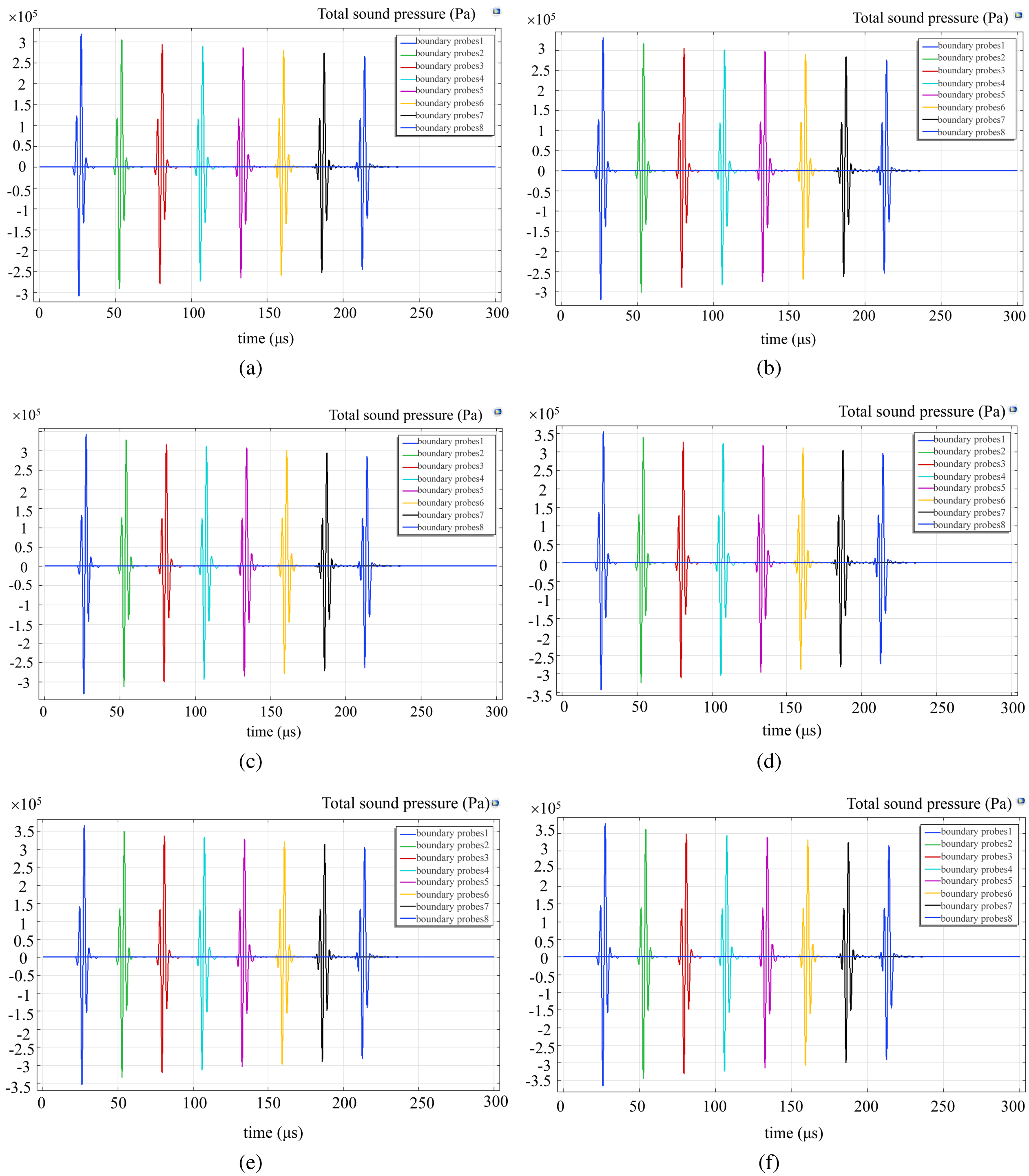

Fig. 10. Ultrasonic pressure waveforms obtained from probe detection under different drilling fluid densities. (a) 1.08 g/cm^3, (b) 1.12 g/cm^3, (c) 1.16 g/cm^3, (d) 1.20 g/cm^3, (e) 1.24 g/cm^3 and (f) 1.28 g/cm^3.

Table 2. Ultrasonic sound pressure data detected by probes Nos.1-8 at different ultrasonic frequencies.

Frequency (MHz)	Pressure at different transmission distance ($\times 10^5$ Pa)							
	30 (mm)	70 (mm)	110 (mm)	150 (mm)	190 (mm)	230 (mm)	270 (mm)	310 (mm)
0.1	1.11997	1.07485	0.99923	0.97619	0.96908	0.95074	0.92002	0.88261
0.2	2.29654	2.21928	2.20923	2.15594	2.08472	2.02752	1.98577	1.93473
0.3	3.43836	3.27237	3.15525	3.11974	3.07624	3.01593	2.93804	2.85368
0.4	4.60346	4.38555	4.20174	4.06469	4.01914	3.97808	3.91420	3.84240
0.5	5.73976	5.42065	5.16457	4.89608	4.71840	4.64127	4.57456	4.47926
0.6	6.88614	6.47244	6.13632	5.84213	5.53026	5.35090	5.26193	5.18584

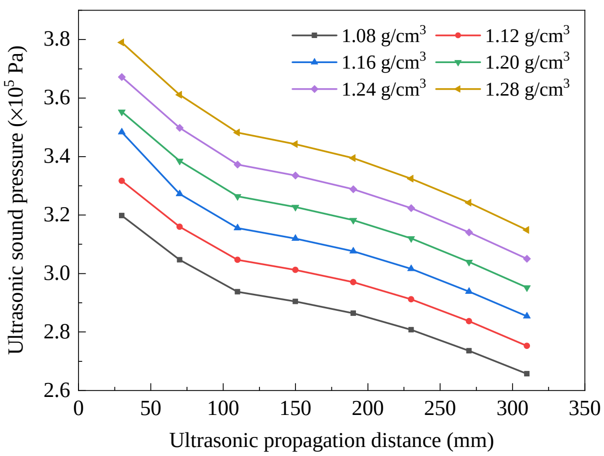

Fig. 11. Ultrasonic sound pressure data detected by Nos.1-8 probes.

gation, mm; $y_1 \sim y_6$ represents the sound pressure of the ultrasonic wave, 10^5 Pa.

It can be seen that as the frequency of the ultrasonic wave increases, the absolute value of the slope of the ultrasonic fitting curve also increases, indicating that the attenuation of ultrasonic wave increases, that is, the greater the ultrasonic frequency, the faster the attenuation.

4. Laboratory test

During its propagation in the water-based drilling fluid, the ultrasonic wave will attenuate. In the indoor experiment, ultrasonic waves of 0.1, 0.2, 0.3, 0.4, 0.5 and 0.6 MHz frequencies are considered for testing. The detection device is set during propagation, and the ultrasonic pressure data received by the ultrasonic wave propagation here is used to determine the energy attenuation of the ultrasonic wave. The experimental system consists of a signal generator, power amplifier (HSA4101), oscilloscope, industrial computer, ultrasound probe, among other components. The signal generator outputs the signal to the power amplifier and the power amplifier outputs the signal to drive the ultrasonic probe. The connection mode of the ultrasonic probe is illustrated in Fig. 14.

The CN2R-24 contact ultrasonic probe, as a high-performance ultrasonic transducer, is widely used in industrial and medical fields of ultrasonic detection, therefore it is also used in this experiment. Firstly, the ultrasonic probes are attached to the inner surface of the sink, with an interval of 40 mm between each two. The water-based drilling fluid with 1.16 g/cm^3 is poured into the sink and the 0.3 MHz ultrasonic signal is emitted by the signal generator, indicating that the ultrasonic wave has been transmitted through the water-based drilling fluid. The test principle is shown in Fig. 15. The ultrasonic sound pressure signal received by the probe is displayed on the oscilloscope, and the propagation characteristics of ultrasonic wave in water-based drilling fluid are studied by observing the waveforms of ultrasonic probes at different positions on the oscilloscope.

From the waveform of the oscilloscope during the experiment, as the propagation distance increases, the ultrasonic sound pressure detected by the latter probe has a certain attenuation compared with the previous probe, which means that the ultrasonic wave gradually attenuates. When 0.1, 0.2, 0.4, 0.5 and 0.6 MHz ultrasonic waves are emitted by the signal generator, by observing the waveforms on the oscilloscope at different frequencies, it is concluded that with the increase in ultrasonic frequency, the difference in ultrasonic sound pressure detected by two adjacent probes is greater, that is, with the higher the ultrasonic frequency, the faster the ultrasonic attenuation.

5. Conclusions

In this work, by constructing a theoretical model and performing numerical simulation and laboratory tests, the propagation characteristics of ultrasonic wave in water-based drilling fluid and its attenuation law of scattering and viscosity were explored. The main conclusions are as follows:

1) The combination of theoretical and numerical simulation is of great value for studying the propagation characteristics of ultrasonic wave in water-based drilling fluid. The results were verified by the indoor test results, which underscores the potential of this strategy in exploring the propagation characteristics of ultrasonic wave in water-based drilling fluid.
2) By comparing the scattering and viscous attenuation coefficients, it was found that the former is much larger than the latter, and that the main type of ultrasonic attenuation

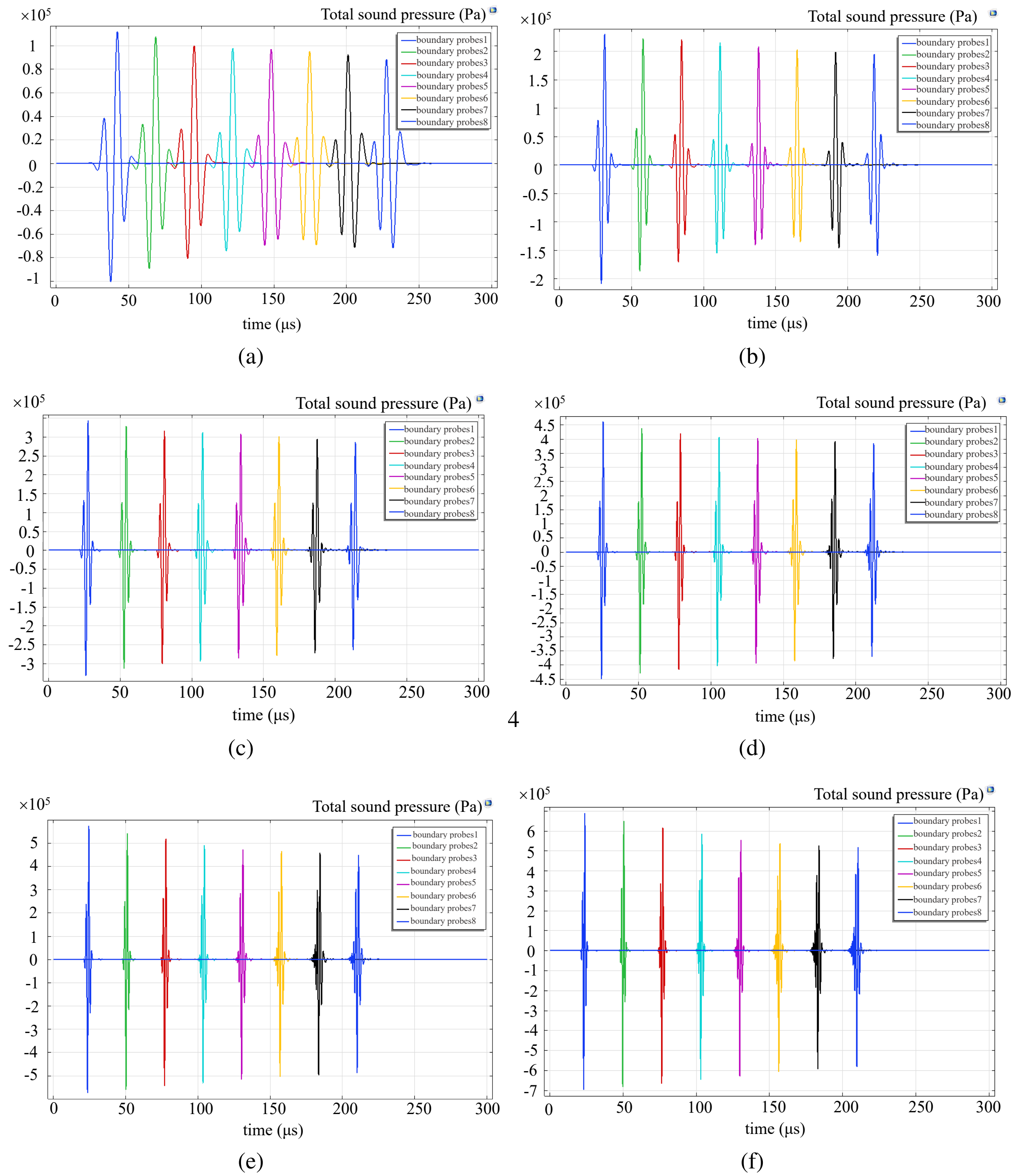

Fig. 12. Ultrasonic pressure waveforms of probe detection under different ultrasonic frequencies. (a) 0.1 MHz, (b) 0.2 MHz, (c) 0.3 MHz, (d) 0.4 MHz, (e) 0.5 MHz and (f) 0.6 MHz.

is scattering attenuation.

3) When the density of drilling fluid and ultrasonic frequency are constant, the ultrasonic attenuation rate in the water-based drilling fluid is positively correlated with the solid particle size, solid particle number and ultrasonic frequency, while it is negatively correlated with the density of water-based drilling fluid. Furthermore, the ultrasonic energy decreases with the increase in propagation distance.
4) The above conclusions can improve the accuracy of ultrasonic flowmeter to monitor the annular return flow rate of drilling fluid at the wellhead, enhance the efficiency of field operation and the success rate of drilling, and have certain guiding significance for the development of intelligent drilling system. As a limitation of this study, the internal structure of the wellbore, ultrasonic reflection and the influence of space were not taken into account. Going forward, more in-depth research is needed to develop and better utilize the ultrasonic measurement technology, with the ultimate aim of accurately measuring the drilling fluid annular return flow rate.

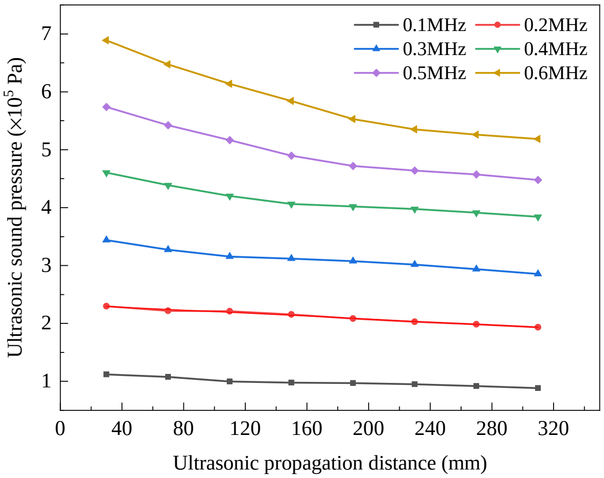

Fig. 13. Ultrasonic sound pressure data detected by probes No.1-8 probe at different ultrasonic frequencies.

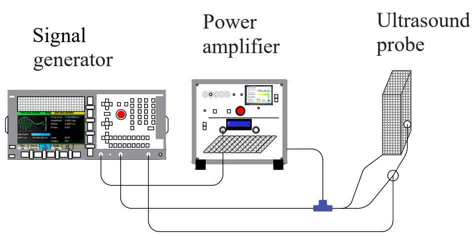

Fig. 14. Connection mode of the ultrasound probe.

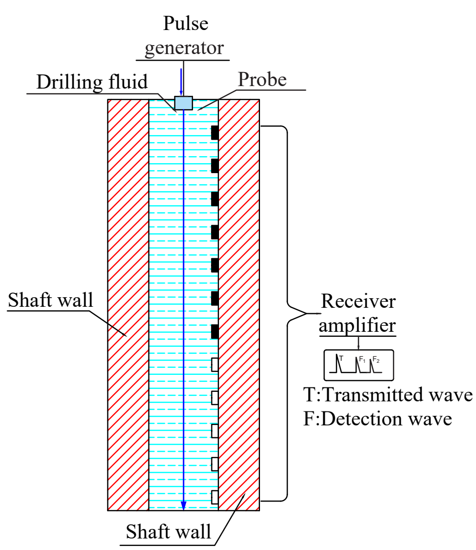

Fig. 15. Schematic diagram of the experiment.

Acknowledgements

The authors would like to express their sincere gratitude for the support provided by the China Energy Digital Technology Group Limited, as well as Yangtze University.

Conflict of interest

The authors declare no competing interest.

References

Allegra, J. R., Hawley, S. A. Attenuation of sound in suspensions and emulsions: Theory and experiments. The Journal of the Acoustical Society of America, 1972, 51(5B): 1545-1564.

Broni-Bediako, E., Amorin, R. Experimental study on the effects of cement contamination in a water based mud. Advances in Geo-Energy Research, 2019, 3(3): 314-319.

Chen, Q., Xu, F., Cheng, L., et al. Shale ultrasonic numerical simulation based on the viscoelastic medium wave theory. Natural Gas Industry, 2019, 39(6): 63-70. (in Chinese)

Chen, Q., Yao, G., Zhu, H., et al. Numerical simulation of ultrasonic wave transmission experiments in rocks of shale gas reservoirs. Aip Advances, 2017, 7(1): 015205.

Citarella, R., Federico, L., Cicatiello, A. Modal acoustic transfer vector approach in a FEM-BEM vibro-acoustic analysis. Engineering Analysis with Boundary Elements, 2007, 31(3): 248-258.

Fan, J., Wang, F. Review of ultrasonic measurement methods for two-phase flow. Review of Scientific Instruments, 2021, 92(9): 091502.

Ge, Y. Mei, Y., Zhang, S., et al. Development of online drilling fluid property logging system. Paper SPE 208694 Presented at the IADC/SPE International Drilling Conference and Exhibition, Galveston, Texas, USA, 8-10 March, 2022.

Holt, R. M., Larsen, I., Fjær, E., et al. Comparing mechanical and ultrasonic behaviour of a brittle and a ductile shale: Relevance to prediction of borehole stability and verification of shale barriers. Journal of Petroleum Science and Engineering, 2020, 187: 106746.

Indimath, S., Bøklepp, B. R., Måsøy, S. E. Performance of Doppler ultrasound for fluid influx/efflux velocity estimation from borehole fractures in water-based and oil-based muds. Geoenergy Science and Engineering, 2024, 239: 212903.

Ismail, A. R. Improve performance of water-based drilling fluids. Paper Presented at the 5th Sriwijaya International Seminar on Energy and Environmental Science and Technology, Palembang, Indonesia, 10-11 September, 2014.

Jia, H., Wang, C., Dang, R. The influence of fluid flow rate on the accuracy of ultrasonic flow measurement and its calibration. Journal of Instrumentation, 2020, 41(7): 1-8. (in Chinese)

Korlapati, N. V. S., Khan, F., Noor, Q., et al. Review and analysis of pipeline leak detection methods. Journal of pipeline science and engineering, 2022, 2(4): 100074.

Kuang, Z., Yang, W., Lin, H., et al. Research on sediment concentration measurement based on multi-frequency ultrasonic signal response. Measurement, 2023, 208: 112485.

Larrarte, F., François, P. Attenuation of an ultrasonic beam by suspended particles and range of acoustic flow meters in sewer networks. Water Science and Technology, 2012,

65(3): 478-483.
Leśniak, G., Brunner, J., Daniel, et al. Application of long-reach directional drilling boreholes for gas drainage of adjacent seams in coal mines with severe geological conditions. International Journal of Coal Science & Technology, 2022, 9(1): 88.
Li, J., Wan, J., Wang, T., et al. Leakage simulation and acoustic characteristics based on acoustic logging by ultrasonic detection. Advances in Geo-Energy Research, 2022a, 6(3): 181-191.
Li, X., Xue, Y., Du, H., et al. Investigation on leakage detection and localization in gas-liquid stratified flow pipelines based on acoustic method. Journal of Pipeline Science and Engineering, 2022b, 2(4): 100089.
Li, Z., Liu, X., Wang, B., et al. Experimental study and economic evaluation of low temperature drying treatment of abandoned water-based drilling fluid. Coal Geology & Exploration, 2019, 47(4): 201-205. (in Chinese)
Liu, F., Fu, J., Zhang, Z., et al. Research of ultrasonic attenuation theory in drilling fluid. Oil Drilling & Production Technology/Shiyou Zuancai Gongyi, 2012, 34(1): 57-59. (in Chinese)
Ma, H., Zhai, C., Xu, J., et al. Effect of NMR technology-based ultrasonic frequency on stimulated cracking of coal. Coal Geology & Exploration, 2019, 47(4): 38-44. (in Chinese)
Ma, T., Liu, J., Fu, J., et al. Drilling and completion technologies of coalbed methane exploitation: an overview. International Journal of Coal Science & Technology, 2022, 9(1): 68.
Matsushima, J., Suzuki, M., Kato, Y., et al. Estimation of ultrasonic scattering attenuation in partially frozen brines using magnetic resonance images. Geophysics, 2011, 76(1): T13-T25.
Moradi, M. H., Abedini, M. A combination of genetic algorithm and particle swarm optimization for optimal DG location and sizing in distribution systems. International Journal of Electrical Power & Energy Systems, 2012, 34(1): 66-74.
Morse, P. M., Ingard, K. U. Theoretical Acoustics. Princeton, USA, Princeton University Press, 1986.
Mozie, K. N. Characterization of ultrasonic waves in various drilling fluids. Norway, University of South-Eastern Norway, 2017.
Özkök, O. Modeling effects of material properties and composition on ultrasound propagation. Ankara, Middle East Technical University, 2017.
Peruga, H. Y. Ultrasonic interrogation of oil sands tailings during sedimentation. Ottawa, Carleton University, 2021.
Peters, F., Petit, L. Propagation of ultrasound waves in concentrated suspensions. Acta Acustica United with Acustica, 2000, 86(5): 838-846.
Poelma, C. Measurement in opaque flows: A review of measurement techniques for dispersed multiphase flows. Acta Mechanica, 2020, 231(6): 2089-2111.
Seldis, T., Pecorari, C. Scattering-induced attenuation of an ultrasonic beam in austenitic steel. The Journal of the Acoustical Society of America, 2000, 108(2): 580-587.
Setia, G., Mallick, S. S., Pan, R., et al. Modeling minimum transport boundary for fluidized dense-phase pneumatic conveying systems. Powder Technology, 2015, 277: 244-251.
Shahzamanian, M., Lin, M., Kaina, T., et al. Systematic literature review of the application of extended finite element method in failure prediction of pipelines. Journal of Pipeline Science and Engineering, 2021, 1(2): 241-251.
Sheen, S. H., Reimann, K. J., Lawrence, W. P., et al. Ultrasonic techniques for measurement of coal slurry viscosity. Paper Presented at IEEE 1988 Ultrasonics Symposium Proceedings, Chicago, Illinois, 2-5 October, 1988.
Sojahrood, A. J., Li, Q., Haghi, H., et al. Investigation of the nonlinear propagation of ultrasound through a bubbly medium including multiple scattering and bubble-bubble interaction: Theory and experiment. Paper Presented at 2017 IEEE International Ultrasonics Symposium (IUS), Washington, USA, 6-9 September, 2017.
Wang, Z., Zheng, Y. Critical flow velocity phenomenon in erosion-corrosion of pipelines: Determination methods, mechanisms and applications. Journal of Pipeline Science and Engineering, 2021, 1(1): 63-73.
Xia, L., Yw, Y., Wang, X. The Application of ultrasonic guided waves in the furnace tube inspection. Paper V007T07A003 Presented at ASME 2013 Pressure Vessels and Piping Conference, Paris, France, 14-18 July, 2013.
Yasui, K., Kozuka, T., Tuziuti, T., et al. FEM calculation of an acoustic field in a sonochemical reactor. Ultrasonics Sonochemistry, 2007, 14(5): 605-614.
Zhang, S., Qin, L., Li, X., et al. Propagation of Rayleigh waves on curved surfaces. Wave Motion, 2020, 94: 102517.
Zhu, J., Chen, M., Wang, L., et al. Characterization of 10 nm-10 μm coal dust particles generated by simulated different cutting and drilling parameters: Mass concentration distribution, number concentration distribution, and fractal dimension. International Journal of Coal Science & Technology, 2023, 10(1): 89.